

Optimum Experimental Design for EGDM Modeled Organic Semiconductor Devices

C. K. F. Weiler^{1, a)} and S. Körkel¹

Interdisciplinary Center for Scientific Computing (IWR), Heidelberg University, 69120 Heidelberg, Germany.

(Dated: 7 June 2021)

We apply optimum experimental design (OED) to organic semiconductors modeled by the extended Gaussian disorder model (EGDM) which was developed by Pasveer et al.¹ We present an extended Gummel method to decouple the corresponding system of equations and use automatic differentiation to get derivatives with the required accuracy for OED. We show in two examples, whose parameters are taken from Pasveer et al.¹ and Mensfoort and Coehoorn² that the linearized confidence regions of the parameters can be reduced significantly by applying OED resulting in new experiments with a different setup.

PACS numbers: 81.05.Fb,02.60.Lj,02.60.Cb,02.60.Jh,02.60.Pn

Keywords: Organic Semiconductor, Gummel Method, Automatic Differentiation, Optimum Experimental Design, Confidence Region, Covariance Matrix

I. INTRODUCTION

Simulation of organic semiconductor devices, e.g. organic light emitting diodes (OLED), organic solar cells, etc., has gained great interest in the past decade. Accurate models often lack in precise parameters and their identification is time-consuming or expensive. One major problem is the uncertainty in the measurement data which leads to uncertain parameters. Carrying out more experiments would minimize this uncertainty in an expensive way. An alternative is to use OED in order to minimize the parameter uncertainty by planning new (optimal) experiments. New measurement data are received for which the parameter estimation yields parameters with minimal confidence intervals. We apply the concept of OED to the EGDM, a special model for the mobility of electron transport in organic polymeric material. The chapters are arranged as follows: We give a brief overview of the model equations in Sec. II and point out what the relevant quantities are. In Sec. III, we explain the methodology of the optimum experimental design problem in more detail. After describing the equation solver methods we used, Sec. IV, numerical results of the optimization are presented in Sec. V.

II. EGDM EQUATIONS

A basic description of charge transport in semiconducting materials in the steady-state case is given by the coupled van Roosbroeck system³ consisting of the continuity equation, also called drift-diffusion equation, and the Poisson equation. Given a domain $\Omega := (0, L) \subset \mathbb{R}$, the state variables, i.e. the space dependent functions, are the electric charge density n in [m^{-3}] and the electric

potential ϕ in [eV] which are scalar real valued functions defined on Ω . We assume that n and ϕ are twice differentiable on Ω . Pasveer et al.¹ proposed the EGDM to conjugated semi-conducting polymers, where the diffusion and the mobility depend on the state variables and hence on the space variable x . Furthermore they introduced another state E_F , called Quasi-Fermi-Energy, and a corresponding equation which couples E_F and n at every space point. We omit the x -dependence in the following equations, only n , ϕ and E_F are space dependent. The model equations are:

$$0 = \partial_x J(n, \phi, E_F), \quad (1)$$

$$-\partial_x^2 \phi = \frac{e}{\varepsilon} n, \quad (2)$$

$$n = \frac{N_t}{\sqrt{2\pi\sigma^2}} \int_{-\infty}^{\infty} e^{-\frac{E^2}{2\sigma^2}} \frac{1}{1 + \exp\left(\frac{E-E_F}{k_B T}\right)} dE, \quad (3)$$

where

$$J(n, \phi, E_F) = \mu_0 g_0 g_1(n) g_2(\phi) \quad (4)$$

$$\left(n \partial_x \phi - k_B T g_3(n, E_F) \partial_x n \right), \quad (5)$$

$$g_0 = \exp \left\{ -0.42 \left(\frac{\sigma}{k_B T} \right)^2 \right\}, \quad (6)$$

$$g_1(n) = \exp \left[\frac{1}{2} (\hat{\sigma}^2 - \hat{\sigma}) \left(\min \left\{ \frac{2n}{N_t}, 0.2 \right\} \right)^{\delta(\sigma)} \right], \quad (7)$$

$$g_2(\phi) = \exp \left\{ 0.44 (\hat{\sigma}^{\frac{3}{2}} - 2.2) \right\} \quad (8)$$

$$\left[\sqrt{1 + 0.8 \left(\min \left\{ \frac{\partial_x \phi}{N_t^{\frac{1}{3}} \sigma}, 2 \right\} \right)^2} - 1 \right], \quad (9)$$

$$g_3(n, E_F) = \frac{n}{k_B T \frac{dn}{dE_F}}. \quad (10)$$

In these equations J is the electric current density in [$\frac{A}{m^2}$], k_B is the Boltzmann constant in [$\frac{eV}{K}$], ε the permittivity in [$\frac{As}{Vm}$], e the elementary charge in [As], $\hat{\sigma} := \frac{\sigma}{k_B T}$

^{a)}Electronic mail: christoph.weiler@iwr.uni-heidelberg.de

and $\delta(\sigma) := 2^{\frac{\log(\hat{\sigma}-\sigma^2)-\log\log 4}{\hat{\sigma}^2}}$. In the anorganic case, the g_i -factors, $i = 1, 2, 3$, would be constant. Their organic model is yield by comparison with the solution of the master equation.¹ On the boundary $\partial\Omega = \{0, L\}$ the following conditions are imposed:

$$n(0) = \frac{N_t}{\sqrt{2\pi\sigma^2}} \int_{-\infty}^{\infty} e^{-\frac{E^2}{2\sigma^2}} \left[1 + \exp\left(\frac{E + \varphi_1 - \sqrt{\max\left\{-\frac{e}{4\pi\epsilon}\partial_x\phi(0), 0\right\}}}{k_B T}\right) \right]^{-1} dE,$$

$$n(L) = \frac{N_t}{\sqrt{2\pi\sigma^2}} \int_{-\infty}^{\infty} e^{-\frac{E^2}{2\sigma^2}} \frac{1}{1 + \exp\left(\frac{E + \varphi_2}{k_B T}\right)} dE,$$

$$\phi(0) = 0,$$

$$\phi(L) = eV - (\varphi_2 - \varphi_1),$$

where V is the voltage in [V] and $\varphi_{1,2}$ are given energy barriers in [eV]. On the entrance, $x = 0$, the energy barrier φ_1 is lowered according to the theory of Entage and O'Dwyer⁴ and Scott and Malliaras.⁵ For our computations we take the dimensionless form of the equations proposed by Bonham and Jarvis.⁶ For the later use we define

$$p := (\mu_0, \sigma, N_t) \in \mathbb{R}^3,$$

$$q := (L, T) \in \mathbb{R}^2, \quad (11)$$

where p are parameters of unknown numerical value given by nature. They have to be identified by comparing a model response to experimental data. μ_0 is the zero temperature mobility in $[\frac{m^2}{Vs}]$, σ is the width of the Gaussian distribution of the density of states in [eV] and N_t is the site density in $[m^{-3}]$. We assemble quantities which are adjustable by an experimenter, the device length L in [m] and the temperature T in [K], in the vector q .⁷

III. SOLUTION METHODS FOR THE EGDM EQUATIONS

There are two established ways for solving the system (1)-(3):⁸

1. Apply Newton's method to the fully coupled system of equations
2. Use Gummel's method,⁹ i.e. a fixed point iteration which decouples the three EGDM equations

With Newton's method, one can achieve quadratic convergence. However, finding good starting values is not simple. In the work of Knapp et al.,⁸ a strategy motivated by physical considerations is described. Another aspect is that the Jacobian, i.e. derivatives of the functions w.r.t. the states, is required. To compute the Jacobian, the main two options are to use difference formulas or compute the exact derivatives. The latter can be done

TABLE I. Algorithm for the fixed point iteration of Gummel expanded by the EGDM-Quasi-Fermi-Equation and a derivative-free linearization.

Let $u^0 := (n^0, \phi^0, E_F^0)$ be given and choose $\ \Delta u^0\ \gg \text{TOL}$ with given error tolerance TOL.
Set $i = 0$.
while $\ \Delta u^i\ _2 > \text{TOL}$
Solve
$n^i = \frac{N_t}{\sqrt{2\pi\sigma^2}} \int_{-\infty}^{\infty} e^{-\frac{E^2}{2\sigma^2}} \frac{1}{1 + \exp\left(\frac{E - E_F^{i+1}}{k_B T}\right)} dE$
for E_F^{i+1} with Newton's method started with E_F^i .
Solve
$-\partial_x^2 \phi^{i+1} = \lambda n^i$
with corresponding boundary conditions for ϕ^{i+1} .
With n^i, ϕ^{i+1} and E_F^{i+1} solve
$0 = \partial_x \left\{ g_1(n^i) g_2(\phi^{i+1}) \left(n^{i+1} \partial_x \phi^{i+1} - k_B T g_3(n^i, E_F^{i+1}) \partial_x n^{i+1} \right) \right\}$
with corresponding boundary conditions for n^{i+1} .
Set $u^{i+1} := (n^{i+1}, \phi^{i+1}, E_F^{i+1})$ and $\Delta u^{i+1} := u^{i+1} - u^i$.
$i \leftarrow i + 1$

by hand or by using automatic differentiation (AD). Either way, the additional effort for computing the derivative in n directions is at least $2n$ times the effort of each function evaluation in every Newton step. Another possibility is to solve (1)-(3) with Gummel's method. TABLE I shows the modified algorithm consisting of the classical system of equations (1) and (2) and the Quasi-Fermi energy E_F defining equation (3).¹⁰ We solve the equations sequentially and insert the interim results into the next equations. With the special linearization, used in the third equation of TABLE I, we do not need any derivatives and the effort of function evaluations is limited. We discretize the infinite dimensional problem (1)-(3) to a finite one. The domain $\bar{\Omega}$ is divided in N subintervals $I_i := [x_i, x_i + h]$, $x_i \in \{x_0 = 0, \dots, x_N = L\}$ with a constant mesh size $h := \frac{L}{N}$. Finite differences are applied to the spatial derivatives, i.e. with respect to x . The so-called Scharfetter-Gummel scheme¹¹ forces the function J , defined in Eq.(5), to be constant on each interval I_i , denoted by $J_{i+\frac{1}{2}}$, and provides an upwind stabilization, so that computation on coarse meshes is possible. On the interval I_i , the scheme looks like

$$J_{i+\frac{1}{2}} = \mu_0 g_0 \tilde{g}_1 \tilde{g}_2 \frac{\phi_{i+1} - \phi_i}{h} \frac{n_{i+1} \exp\left(-\frac{\phi_{i+1} - \phi_i}{k_B T \tilde{g}_3}\right) - n_i}{\exp\left(-\frac{\phi_{i+1} - \phi_i}{k_B T \tilde{g}_3}\right) - 1}.$$

The terms \tilde{g}_j , $j = 1, 2, 3$ stand for average values of the non-constant functions g_j , $j = 1, 2, 3$. It is important that the averages are taken in an upwind conform way to prevent numerical oscillations.

IV. OPTIMUM EXPERIMENTAL DESIGN FOR MODEL VALIDATION

In this part, we follow the approaches of Lohmann¹² and Körkel et al.¹³ With different choices of the controls q and the voltage V , defined in Sec. II, we set up multiple experiments in which the current density J (5) is measured. Let M be the number of measurements we yield. In a parameter estimation, the parameters are identified by fitting a model response, here J , to experimental data, i.e. measurements. We assume the measurement error to be normally distributed with mean zero and covariance matrix $\Sigma^2 = \text{diag}(\sigma_i^2, i = 1, \dots, M) \in \mathbb{R}^{M \times M}$. With the same experimental settings, i.e. equal controls q , a fit from a different realization of the measurement errors may result in very different parameter values. The covariance matrix of the parameters allows to analyze the quality of a parameter estimation. The assumed model for the standard deviations of the measurement errors is:⁷

$$\sigma_i = 0.1 \cdot \mathcal{J}_i + 0.1 \left[\frac{A}{m^2} \right],$$

where $\mathcal{J}_i \in \mathbb{R}$ is the function value of J corresponding to the i -th measurement. For further notation, we assemble the values \mathcal{J}_i in the vector $\mathcal{J} \in \mathbb{R}^M$. If the confidence region of the parameters is approximated by assuming a linear propagation of the measurement errors, it can be parameterized by the covariance matrix defined by

$$\text{Cov}_p := \mathbb{E}[(p - \mathbb{E}[p])(p - \mathbb{E}[p])^T] \in \mathbb{R}^{N_p \times N_p},$$

where N_p is the number of parameters. From now on, we denote by n , ϕ and E_F the discrete counterparts of the state variables which are $(N - 1)$ -dimensional vectors, without boundary values. They assemble the function values at the mesh points x_i , $i = 1, \dots, N - 1$, cf. Sec.III. We abbreviate the discrete solution of the system (1)-(3) dependent on parameters p and controls q by

$$u(p, q) := (n(p, q), \phi(p, q), E_F(p, q)) \in \mathbb{R}^{N_u},$$

cf. TABLE I. We used the notation $N_u := 3(N - 1)$ for the overall state dimension. In the following we denote the derivative of a function f w.r.t. x in the direction Δx by

$$d_x f\{\Delta x\} := \lim_{\varepsilon \rightarrow 0} \frac{f(x + \varepsilon \Delta x) - f(x)}{\varepsilon}$$

and write accordingly the second derivatives of f w.r.t. x and y in the directions Δx and Δy as $d_{yx}^2 f\{\Delta x, \Delta y\}$. We combine several directions Δx_i into a so-called seed matrix $S = (\Delta x_1, \dots, \Delta x_n)$ and define $d_x f\{S\}$ by

$$(d_x f\{S\})_{ij} = d_x f_i\{\Delta x_j\}$$

and accordingly $d_{yx}^2 f\{S_1, S_2\}$ by

$$(d_{yx}^2 f\{S_1, S_2\})_{ijk} = d_{yx}^2 f_i\{\Delta x_j, \Delta y_k\}$$

with $S_1 = (\Delta x_j)_j$ and $S_2 = (\Delta y_k)_k$. We define the $M \times N_p$ Matrix

$$\begin{aligned} \text{Jac}(u(p, q), p, q) &:= -\Sigma^{-1} d_p \mathcal{J}(u(p, q), p, q) \{I_p\} \\ &= -\Sigma^{-1} \left[\partial_u \mathcal{J} \{ \partial_p u \{ I_p \} \} + \partial_p \mathcal{J} \{ I_p \} \right], \end{aligned}$$

with the derivative of \mathcal{J} w.r.t. to the parameters p with the N_p -dimensional identity matrix I_p as seed matrix. Computing $\partial_u \mathcal{J} \{ \partial_p u \{ I_p \} \}$ is much less expensive than computing the matrix product $\partial_u \mathcal{J} \{ I_u \} \cdot \partial_p u \{ I_p \}$ with the identity matrix $I_u \in \mathbb{R}^{N_u \times N_u}$. The covariance matrix in the unconstrained case can be computed by

$$\text{Cov}_p = (\text{Jac}(u(p, q), p, q)^T \text{Jac}(u(p, q), p, q))^{-1}. \quad (12)$$

For given probability $\alpha \in [0, 1]$ the linearized $(100 \cdot \alpha)\%$ -confidence region is described by

$$G(\alpha, p) = \{v \in \mathbb{R}^{N_p} : v = p + \delta p, \delta p^T \text{Cov}_p^{-1} \delta p \leq \gamma(\alpha)^2\}, \quad (13)$$

with the $(1 - \alpha)$ -quantile of the χ^2 -distribution $\gamma(\alpha)^2$. As an approximation of the confidence intervals of the parameters we use

$$\begin{aligned} [p_i - \theta_i, p_i + \theta_i] \quad \text{with} \\ \theta_i = \gamma(\alpha) \sqrt{(\text{Cov}_p)_{ii}}, \quad i = 1, \dots, N_p. \end{aligned} \quad (14)$$

We point out that for computing Cov_p (and the confidence intervals) no measurement data is necessary. We consider the reduced nonlinear optimization problem

$$\min_q \frac{1}{N_p} \text{trace}(\text{Cov}_p) \quad (15)$$

which is called ‘‘optimum experimental design problem’’. Efficient optimization algorithms require derivative information. For higher order difference formulas, the number of function evaluations increases which can be very costly like in our case. Additionally, low order schemes reduce the number of exact digits, in particular in combination with derivatives of higher order. To avoid such approximation errors, we use automatic differentiation where the derivatives are evaluated up to machine precision. For derivative based optimization, we need the derivative of the gradient of Jac with the seed matrix $I_q \in \mathbb{R}^{N_q \times N_q}$, where N_q is the number of the controls. N_p and N_q are relatively small, so we use the forward mode, where we have to compute

$$\begin{aligned} d_q \text{Jac}(u(p, q), p, q) \{I_q\} \\ &= -\Sigma^{-1} \left[d_q (\partial_u \mathcal{J} \{ \partial_p u \{ I_p \} \} + \partial_p \mathcal{J} \{ I_p \}) \{ I_q \} \right] \\ &= -\Sigma^{-1} \left[\partial_u^2 \mathcal{J} \{ \partial_p u \{ I_p \}, \partial_q u \{ I_q \} \} + \partial_{qu}^2 \mathcal{J} \{ \partial_p u \{ I_p \}, I_q \} \right. \\ &\quad + \partial_u \mathcal{J} \{ \partial_{qp}^2 u \{ I_p, I_q \} \} + \partial_{up}^2 \mathcal{J} \{ I_p, \partial_q u \{ I_q \} \} \\ &\quad \left. + \partial_{qp}^2 \mathcal{J} \{ I_p, I_q \} \right], \end{aligned}$$

see e.g. Griewank.¹⁴ We need derivatives of u w.r.t. the parameters p , controls q and mixed second derivatives w.r.t. p and q . One way would be to differentiate the fixed point iteration, TABLE I, and iterate over the derivatives as well.¹⁵ However, we are only interested in the derivatives of the solution of Gummel's method $u(p, q)$. In the solution it holds

$$F(u(p, q), p, q) = 0 \quad \forall p, q, \quad (16)$$

with F the discrete counterpart of the system of equations (1)-(3). To compute the required derivatives $\partial_p u\{I_p\}$, $\partial_q u\{I_q\}$ and $\partial_{qp}^2 u\{I_p, I_q\}$, we use the sensitivity method, see e.g. Hinze et al.¹⁶ Using adjoint method is not recommended here, because the number of measurements M is much higher than the number of parameters N_p . Differentiating (16) leads to

$$\begin{aligned} d_p F(u(p, q), p, q)\{I_p\} &= 0, \\ d_q F(u(p, q), p, q)\{I_q\} &= 0, \\ d_{qp}^2 F(u(p, q), p, q)\{I_p, I_q\} &= 0. \end{aligned}$$

Hence the required derivatives are given in form of

$$\begin{aligned} \partial_p u\{I_p\} &= -(\partial_u F\{I_u\})^{-1} \partial_p F\{I_p\} \\ \partial_q u\{I_q\} &= -(\partial_u F\{I_u\})^{-1} \partial_q F\{I_q\} \\ \partial_{qp}^2 u\{I_p, I_q\} &= -(\partial_u F\{I_u\})^{-1} \left(\partial_{qp}^2 F\{I_p, I_q\} \right. \\ &\quad + \partial_{up}^2 F\{I_p, \partial_q u\{I_q\}\} + \partial_{qu}^2 F\{\partial_p u\{I_p\}, I_q\} \\ &\quad \left. + \partial_u^2 F\{\partial_p u\{I_p\}, \partial_q u\{I_q\}\} \right). \end{aligned} \quad (17)$$

We can save the decomposition of the matrix $\partial_u F\{I_u\}$ and use it for all three equations to reduce complexity.

V. NUMERICAL RESULTS

Experimenters proceed in the following way.¹⁷ Devices of different lengths L are produced by evaporating. At different temperatures T , they apply voltage series \mathcal{V} , a vector consisting of various voltages V , and measure the corresponding current values, combined in the vector \mathcal{J} . One choice of L , T and voltage series \mathcal{V} we call one experiment subsequently. We will show in two examples how the confidence regions (13) can be reduced by OED. In each example we consider three different lengths

$$\mathcal{L} := (L_1, L_2, L_3)$$

and three different temperatures

$$\mathcal{T} := (T_1, T_2, T_3).$$

The combination of each element of the vector \mathcal{L} with each element of the vector \mathcal{T} lead to nine experiments. We assemble all control variables, which are the optimization variables for the OED problem, in a vector

$$\mathcal{Q} := (L_1, T_1, L_1, T_2, L_1, T_3, L_2, T_2, \dots, L_3, T_3) \in \mathbb{R}^{18}.$$

The result of the OED should be three lengths and three temperatures combined in nine experiments. To enforce that, we apply additional constraints to \mathcal{Q} for the lengths

$$\begin{aligned} \mathcal{Q}_1 &= \mathcal{Q}_3 = \mathcal{Q}_5, \\ \mathcal{Q}_7 &= \mathcal{Q}_9 = \mathcal{Q}_{11}, \\ \mathcal{Q}_{13} &= \mathcal{Q}_{15} = \mathcal{Q}_{17}, \end{aligned}$$

and for the temperatures

$$\begin{aligned} \mathcal{Q}_2 &= \mathcal{Q}_8 = \mathcal{Q}_{14}, \\ \mathcal{Q}_4 &= \mathcal{Q}_{10} = \mathcal{Q}_{16}, \\ \mathcal{Q}_6 &= \mathcal{Q}_{12} = \mathcal{Q}_{18}. \end{aligned}$$

We solve problem (15) with the software package *VPLAN*¹⁸ where the optimization problem is solved with an inexact SQP method provided by *SNOPT 7.2-9 (Jun 2008)*.¹⁹ In each iteration, the objective, i.e. the covariance matrix, is computed by solving the underlying system of equations. We implemented the extended Gummel method TABLE I in *VPLAN* to solve this system. For the optimization, the derivatives of the model functions are calculated with the AD tool *ADIFOR 2.0*.²⁰ We implemented a routine in *VPLAN*, which solves the system of equations (17). In a first example we take configurations p , \mathcal{V} , \mathcal{L} and \mathcal{T} from Pasveer et al.¹ who used

$$\begin{aligned} p &= (1.15 \cdot 10^{-5}, 0.14, 2.44 \cdot 10^{26}), \\ \mathcal{V} &= (0.1, \dots, 0.9, 1, 2, \dots, 10), \\ \mathcal{L} &= (275, 350, 475), \\ \mathcal{T} &= (235, 270, 305). \end{aligned} \quad (18)$$

Here and in the following example we set $\varphi_1 = \varphi_2 = 0$ for the energy barriers in [eV] and $\varepsilon = 2.66 \cdot 10^{-11}$ for the permittivity in [$\frac{As}{Vm}$]. We choose boundaries to the lengths and temperatures according to the practicability of experiments and the validity of the model:

$$L_i \in [50, 500] \quad \text{and} \quad T_i \in [200, 350] \quad i = 1, 2, 3. \quad (19)$$

The optimization results in the vectors

$$\begin{aligned} \mathcal{L}^* &= (50, 339.1, 471.6), \\ \mathcal{T}^* &= (277.2, 281.8, 350). \end{aligned}$$

Where the lengths do not change much, a tendency to higher temperatures is observed. The algorithm gives back the exact numbers of the optimum. Dependent on the equipment of the laboratory these values can not be realized in practice. Nevertheless they can be taken as a guideline. All the values in the neighborhood of \mathcal{L}^* and \mathcal{T}^* are leading to similar results. In Fig. 1, we visualize the three dimensional ellipsoid and the projections corresponding to the set $G_L(0.95, 0)$ before and after the optimization. TABLE II shows a comparison of the confidence intervals of the parameters. The average of the squared semi-axes of the optimized ellipsoid, i.e. the objective in (15), is 0.07 times the average of the squared

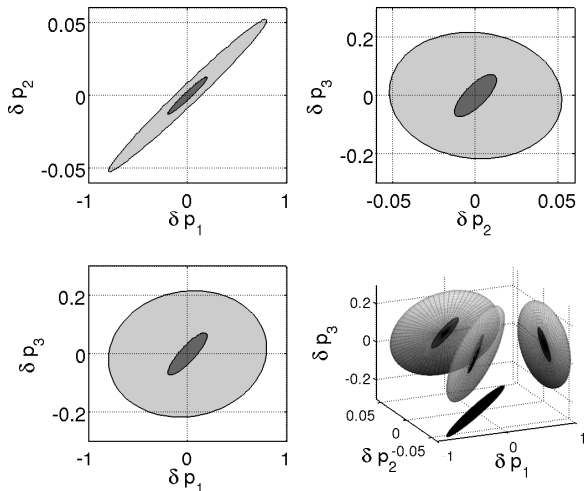


FIG. 1. Projections and three dimensional ellipsoid with shadows of the linearized 95%-confidence regions before (light part) and after (dark part) the optimization. Computed with Pasveer parameters (18).

TABLE II. Radii of the confidence intervals before and after the optimization computed by (14) with Pasveer parameters (18).

	θ_{start}	θ_{optimal}
p_1	79.90%	19.85%
p_2	5.21%	1.27%
p_3	21.62%	7.21%

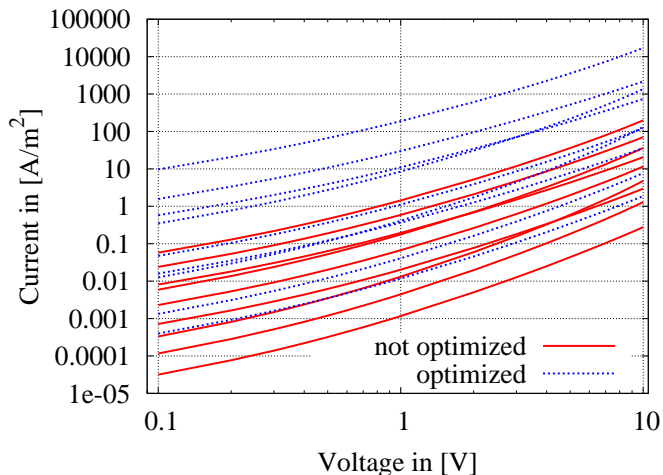


FIG. 2. Comparison of current-voltage characteristics before and after the optimization for Pasveer parameters (18). The continuous lines correspond to experiments with configuration \mathcal{L} and \mathcal{T} and the dashed lines correspond to experiments with optimal configuration \mathcal{L}^* and \mathcal{T}^* .

semi-axes of the ellipsoid not optimized. The results of the simulations before and after the optimization procedure are shown in Fig. 2. The optimal configuration leads to higher current densities. A second example is taken from Mensfoort and Coehoorn,² who used

$$\begin{aligned}
 p &= (1.0 \cdot 10^{-10}, 0.077, 4.25 \cdot 10^{26}), \\
 \mathcal{V} &= (0.1, \dots, 0.9, 1, 2, \dots, 10), \\
 \mathcal{L} &= (100, 200, 300), \\
 \mathcal{T} &= (235, 270, 305).
 \end{aligned} \tag{20}$$

Again we take boundaries like in (19) and the resulting vectors are

$$\begin{aligned}
 \mathcal{L}^* &= (50, 187.8, 296.8), \\
 \mathcal{T}^* &= (200, 274.7, 350).
 \end{aligned}$$

Unlike the first example, the optimal lengths differ much more from the starting values and not all temperatures were raised, the lowest temperature was even reduced. In Fig. 3, we illustrate the confidence ellipsoid and the projections and TABLE III shows a comparison of the con-

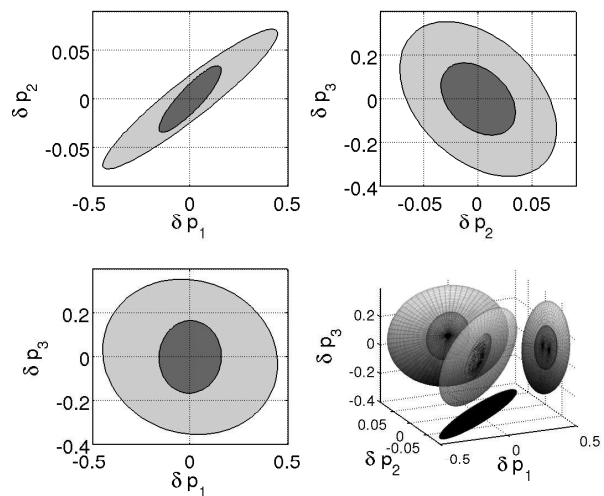


FIG. 3. Projections and three dimensional ellipsoid with shadows of the linearized 95%-confidence regions before (light part) and after (dark part) the optimization. Computed with Coehoorn parameters (20).

fidence intervals in this case. The average of the squared semi-axes of the optimized ellipsoid here is 0.16 times the average of the squared semi-axes of the ellipsoid not optimized, too. The results of the simulations before and after the optimization procedure are shown in Fig. 4. The optimized configuration leads to a wider range of current densities gaining more information.

VI. CONCLUSION AND OUTLOOK

We have applied optimum experimental design to organic semiconductors modeled by the EGDM in order

TABLE III. Radii of the confidence intervals before and after the optimization computed by (14) with Coehoorn parameters (20).

	θ_{start}	θ_{optimal}
p_1	44.76%	15.98%
p_2	7.20%	3.42%
p_3	35.42%	16.51%

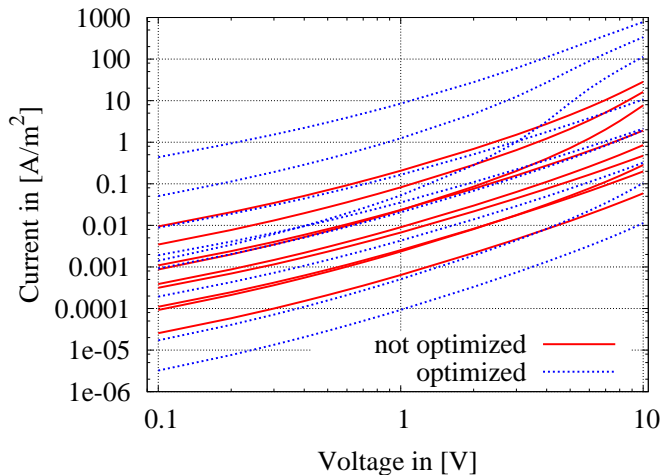


FIG. 4. Comparison of current-voltage characteristics before and after the optimization for Pasveer parameters (20). The continuous lines correspond to experiments with configuration \mathcal{L} and \mathcal{T} and the dashed lines correspond to experiments with optimal configuration \mathcal{L}^* and \mathcal{T}^* .

to reduce the parameter uncertainty caused by measurement errors. The variances of the parameters, i.e. the average of the squared semi-axes of the confidence ellipsoid, were 0.07 and 0.16 times the average of the squared semi-axes of the not optimized confidence ellipsoid respectively. The proposed experiments, followed by a parameter estimation lead to a model, which is approximately 10 times more exact with respect to the assumed measurement error than the previous one. The classical methods for solving semiconductor models were extended to fit with the EGDM. The derivatives required for the optimization were computed via automatic differentiation, leaving the error on machine precision level, even for higher derivatives. We used unipolar layer devices for simplicity, but the presented methods can also be applied to multi-layer devices, trap generation models and exciton rate equations or, more

far-reaching, all other models which are based on the van Roosbroeck system.

ACKNOWLEDGMENTS

The authors acknowledge financial support from the German Federal Ministry of Education and Research (BMBF), project PARAPLUE 03MS649A.

- ¹W. F. Pasveer, J. Cottaar, C. Tanase, R. Coehoorn, P. W. M. B. P. A. Bobbert, D. M. de Leeuw, and M. A. J. Michels, *Phys. Rev. Lett.* **94** (2005).
- ²S. L. M. van Mensfoort and R. Coehoorn, *Phys. Rev. B* **78** (2008).
- ³W. van Roosbroeck, *Bell System Tech* **29**, 560 (1950).
- ⁴P. Emtage and J. J. O'Dwyer, *Phys. Rev. Lett.* **16**, 356 (1966).
- ⁵J. C. Scott and G. G. Malliaras, *Chem. Phys. Lett.* **299**, 115 (1999).
- ⁶J. Bonham and D. Jarvis, *Aust. J. Chem.* **30**, 705 (1977).
- ⁷A. Badinski, (2011), private communication, BASF SE Ludwigshafen.
- ⁸E. Knapp, R. Häusermann, H. U. Schwarzenbach, and B. Ruhstaller, *Journal of applied physics* **108** (2010).
- ⁹H. K. Gummel, *IEEE Trans. Electron Devices* **11**, 455 (1964).
- ¹⁰S. Stodtmann, R. M. Lee, C. K. F. Weiler, and A. Badinski, "Numerical simulation of organic semiconductor devices with high carrier densities," *Journal of applied physics* (2012), submitted, arXiv:1208.3365 [physics.comp-ph].
- ¹¹D. L. Scharfetter and H. K. Gummel, *IEEE Trans. Electron Devices* **16**, 64 (1969).
- ¹²T. Lohmann, H. Bock, and J. Schlöder, "Numerical methods for parameter estimation and optimal experimental design in chemical reaction systems," *Industrial and Engineering Chemistry Research* **31**, 54–57 (1992).
- ¹³I. Bauer, H. Bock, S. Körkel, and J. Schlöder, "Numerical methods for optimum experimental design in DAE systems," *J. Comput. Appl. Math.* **120**, 1–15 (2000).
- ¹⁴A. Griewank, *Evaluating Derivatives, Principles and Techniques of Algorithmic Differentiation*, *Frontiers in Applied Mathematics* No. 19 (SIAM, Philadelphia, 2000).
- ¹⁵B. Christianson, "Reverse accumulation and attractive fixed points," *Optim. Methods Soft.* **3**, 311–326 (1994).
- ¹⁶M. Hinze, R. Pinnau, M. Ulbrich, and S. Ulbrich, *Optimization with PDE Constraints*, *Mathematical Modelling: Theory and Applications* (Springer, 2010).
- ¹⁷M. Al-Helwi, (2011), private communication, BASF SE Ludwigshafen.
- ¹⁸S. Körkel, *Numerische Methoden für Optimale Versuchsplanungsprobleme bei nichtlinearen DAE-Modellen*, Ph.D. thesis, Universität Heidelberg, Heidelberg (2002).
- ¹⁹P. Gill, W. Murray, and M. Saunders, "Snopt: An SQP algorithm for large-scale constrained optimization."
- ²⁰C. Bischof, P. Khademi, and A. Mauer, "The ADIFOR 2.0 system for the automatic differentiation of Fortran 77 programs," Technical Report CRPC-TR94491 (Center for Research on Parallel Computation, Rice University, Houston, TX, 1994).